

# 2D Inversion of Magnetic Anomaly data based on Deep Learning

Haokang Yang  
 School of Electric Information and  
 Electrical Engineering  
 Yangtze University  
 Jingzhou, China

Jie Xiong  
 School of Electric Information and  
 Electrical Engineering  
 Yangtze University  
 Jingzhou, China

Yicheng Cao  
 School of Electric Information and  
 Electrical Engineering  
 Yangtze University  
 Jingzhou, China

**Abstract:** This Magnetic exploration is a geophysical exploration method to study geological structure and mineral resources. Inversion is an effective method to estimate the horizontal location, depth, and geometry of subsurface geological bodies. To resolve the problems of traditional inversion methods, such as dependence on initial model and long calculation time, we proposed a 2D inversion method of magnetic anomaly data based on Deep Learning. With this method, a number of magnetic anomalous body models were designed to perform forward simulation, which generated sample dataset, firstly; a new convolution neural network (CNN) magnetic inversion network was designed, secondly; the sample dataset was used to train the network thirdly; and inversion experimental was performed to evaluate the proposed method lastly. The experimental results show that the proposed method can invert position and magnetization of magnetic anomaly, with strong learning ability and certain generalization ability, and can solve the magnetic inversion problem effectively.

**Keywords:** Magnetic Anomaly; 2D inversion; Deep Learning; convolution neural network (CNN)

## 1. INTRODUCTION

Magnetic exploration is an important geophysical exploration method, which is based on the magnetic differences of rocks, minerals, and other media in the crust [1]. It is a geophysical method that explores geological structures and seeks mineral resources by observing the changes in magnetic field data. Magnetic anomaly inversion is an essential method for quantitatively interpreting magnetic data [2]. Traditional linear iterative regularization inversion is prone to getting stuck in local minima, and global optimization inversion methods have received widespread attention. Nonlinear methods such as Monte Carlo (MC) [3], simulated annealing (SA) [4], genetic algorithm (GA) [5], artificial neural network (ANN) [6], particle swarm optimization (PSO) [7], differential evolution [8], ant colony optimization (ACO) [9] have been widely used in geophysical inversion.

Deep learning has been a research hotspot in the field of artificial intelligence in recent years, and has been widely applied in fields such as computer vision and natural language processing [10]. In recent years, deep learning has been introduced into the field of geophysical inversion. However, the applications in the field of gravity and magnetic inversion are limited [2, 11-12]. Further research is needed on how to design suitable network structures [12]. Therefore, this article proposes a 2D inversion method of magnetic anomaly based on Deep Learning, in order to achieve better inversion results.

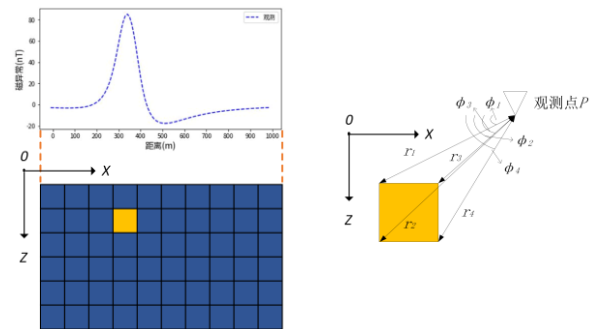
## 2. Methodology

### 2.1 Forward and Inversion modelling

#### (1) Magnetic Forward modelling

Divide the underground into many regular and uniform cell sizes (the blue part represents the mesh of the division, and the yellow part represents the anomaly geological body). When the residual magnetization of a geological body is very small, residual magnetization may usually not be considered. At this time, the magnetization intensity  $\vec{M}$  is equal to the induced magnetization intensity  $\vec{Mi}$ . When the vertical

component response of an infinite strike and finite depth thick plate body is forward modeled, the magnetic anomaly is :



(a) global schematic diagram (b) local schematic diagram

Figure. 1 2D prism forward modelling schematic diagram

$$F = \kappa F_e G \quad (1)$$

$$G = 2 \left[ \cos I \sin \beta \ln \frac{r_2 \cdot r_3}{r_1 \cdot r_4} - \sin I \left[ (\phi_1 - \phi_2) - (\phi_3 - \phi_4) \right] \right],$$

where  $\kappa$  is the magnetic susceptibility,  $F_e$  is the strength of the geomagnetic field,  $I$  is magnetic inclination angle,  $\beta$  is the magnetic north angle,  $r_i$  is the distance,  $\phi_i$  is the angle with respect to the horizontal direction.

Forward modelling can be also described as following:

$$\mathbf{d} = \mathbf{Gm} \quad (2)$$

Where  $\mathbf{m}$  is geological body model, represented as

$\mathbf{m} = [m_1, m_2, m_3, \dots, m_L]^T$ ,  $\mathbf{d}$  is observed data present-

ed as  $\mathbf{d} = [d_1, d_2, d_3, \dots, d_N]^T$ ,  $\mathbf{G}$  is the kernel matrix.

## (2) Magnetic Inversion modelling

Inversion modelling is the process of finding a magnetization model of a geological body and making its predicted magnetic anomaly fitting the observed magnetic anomaly as better as possible. Therefore, the data fitness objective function is defined as following:

$$f(\mathbf{m}) = \|\mathbf{d} - \mathbf{Gm}\|^2 \rightarrow 0 \quad (3)$$

where  $\mathbf{d}$  is observed magnetic anomaly data,  $\mathbf{m}$  is the predicted model,  $\mathbf{Gm}$  is the predicted data.

## 2.2 Inversion Method

Our 2D inversion method of magnetic anomaly data based on deep learning can be described as Figure. 2. The inversion include four steps: (1) design various geological body magnetization intensity models and compute the observed data by forward modelling; (2) combining the models and observed data as training dataset to train the CNN; (3) when training finished, a trained CNN is obtained; (4) input the new observed data input CNN, obtain the predicted model.

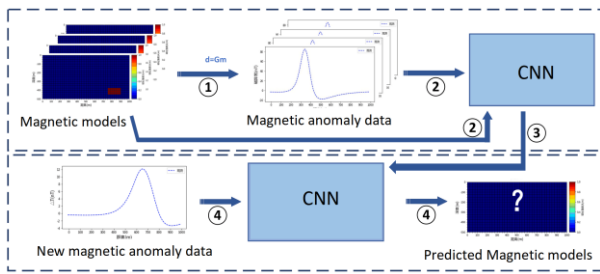


Figure. 2 Inversion method diagram

## 2.3 Network Structure

According to the observation points and the dissected underground space, the input layer of the network contains 101 neurons, and the output layer contains 800 neurons. There are three types in between: Convolutional Layer (CONV), Maximum Pooling Layer (POOL), and Fully Connected Layer. There are four convolutional layers, each of which is followed by a pooling layer. The last hidden layer is a fully connected layer containing 1600 neurons, and the input of this fully connected layer is obtained by flattening the output matrix of the last convolutional pooling layer. Specifically, the four convolutional layers have kernel sizes of  $1 * 5$ ,  $1 * 4$ ,  $1 * 3$ , and  $1 * 3$ , each with a step size of 1. The number of channels is 10, 20, 40, and 80, respectively; All maximum pooling layers have a pooling kernel size of  $1 * 2$  and a step size of 1. The inversion convolution neural network(CNN) illustrated as figure 3.

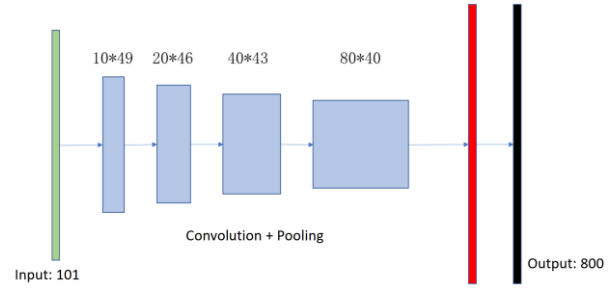


Figure. 3 Inversion Network structure

## 3. Experimental Results

### 3.1 Training Dataset

When setting up the training set samples, we divided the observed underground space into 800 (20 rows  $\times$  40 columns) rectangular cells, each cell size is  $25\text{m} \times 25\text{m}$ . In the forward modeling, 101 ground observation points are set with a spacing of 10m between them. The training dataset contains gravity anomaly bodies of different sizes, shapes (squares, rectangles), and positions, such as  $3 \times 3$  ( $75\text{m} \times 75\text{m}$ ),  $4 \times 4$  ( $100\text{m} \times 100\text{m}$ ),  $5 \times 5$  ( $125\text{m} \times 125\text{m}$ ),  $3 \times 6$  ( $75\text{m} \times 150\text{m}$ ),  $6 \times 3$  ( $150\text{m} \times 75\text{m}$ ),  $4 \times 8$  ( $100\text{m} \times 200\text{m}$ ),  $8 \times 4$  ( $200\text{m} \times 100\text{m}$ ). To prevent the influence of edge data on experimental errors, we discard the data from two units near the edge of the underground grid and only retain the data from the middle part. Due to the linear relationship between magnetic susceptibility and magnetic anomalies, the network can easily learn this linear relationship. Therefore, only two different values (50A/m and 100 A/m) are set for the magnetic anomaly bodies. 5542 sets of underground magnetic models and their corresponding surface observation magnetic anomaly data were generated through forward modeling of anomalies. Figure 4 shows six representative forward models in the dataset.



Figure. 4 Differential forward models.

### 3.2 Training Parameters Setting

Validate set contains 1109 samples extracted from the original 5542 data samples, while the training set contains the remained 4433 samples. The settings for other network parameters are shown in Table 1.

Table. 1 Sample dataset and network parameters setting

	Name	Values
Sample dataset	Training set	4433
	Validate set	1109
Network settings	Learning rate	$\eta=0.0001$
	Activate function	ReLU
	Optimizer	Adam
	L2 regular	$\lambda=0.01$
	Dropout	1

Training process	Iteration	50000
	Batch size	1000

### 3.3 Single anomaly body experiment

the inversion results of the samples in the validate set are shown in Figure 5, with different colors representing different densities, a white box displaying the true position of the model, a blue dashed line representing the actual gravity anomaly, and a red solid line representing the predicted theoretical magnetic susceptibility anomaly obtained from the forward modeling of the underground magnetic susceptibility model. It could be found that the predicted magnetic susceptibility of individual positions of some gravity anomaly bodies is lower than the actual value, and there is a small amount of scattered anomaly information around them, but it does not affect the determination of the center position and overall shape of the magnetic anomaly bodies.

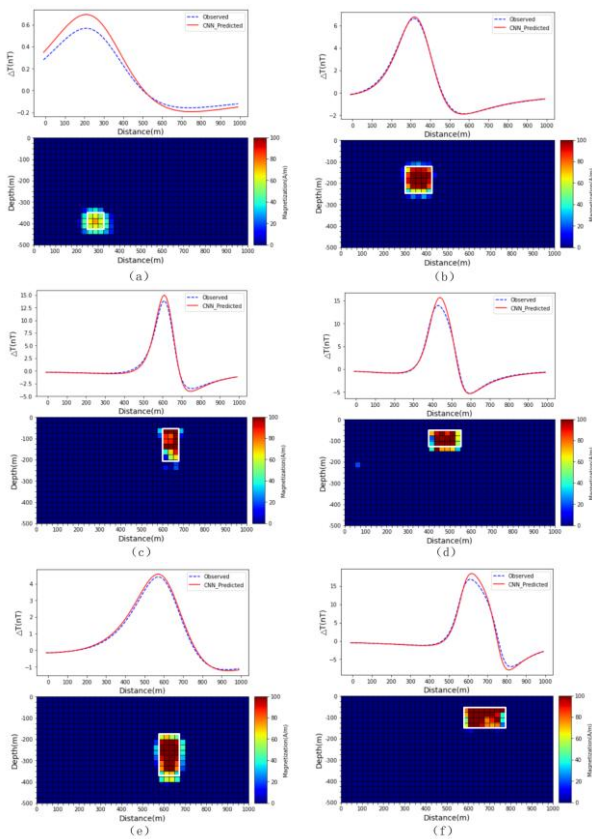


Figure. 5 Inversion results of single anomaly body

### 3.4 Combination anomaly bodies experiment

Figures 6 shows the CNN inversion results of six combination anomaly bodies models. The inversion results of the models show high resolution. For example, single prism and two parallel rectangular prisms can be restored very well, which are shown in Figures 6 (a) (c). Due to the presence of false anomalies, the boundaries of stepped prisms become difficult to distinguish, such as one stepped prism and two stepped prisms, which are shown in Figure 6(b)(d)(e). Moreover, there is distortion phenomenon, and there is a

significant difference in the inversion magnetization intensity, which can reach 100A/m in some places. The magnetization intensity distribution of vertically separated prisms has a low vertical resolution, shown in Figure 6(f), which may be connected to shallow layers and fail to separate well.

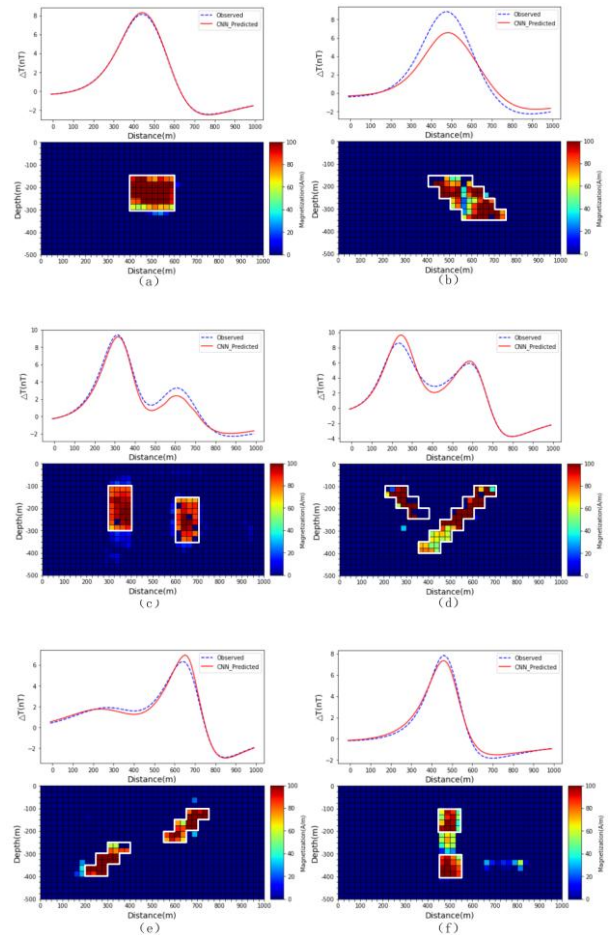


Figure. 6 Inversion results of combination anomaly bodies

## 4. CONCLUSION

This article proposes a deep learning based magnetic anomaly inversion method. Firstly, a CNN inversion network is designed for magnetic anomaly inversion. Then, a large number of magnetic anomaly body models are designed and labeled datasets are obtained through forward calculation. Secondly, the CNN inversion network is trained using this labeled dataset. Finally, the magnetic anomaly data is input into the trained CNN inversion network to directly obtain the inversion results. The experimental results show that this method can invert the position and magnetic susceptibility of anomalous bodies correctly, has good generalization ability and noise resistance, and can effectively solve the problem of magnetic anomaly inversion. Deep learning has been preliminarily applied in magnetic anomaly inversion, and the next works will focus on how to design better network structures to solve three-dimensional magnetic anomaly inversion problems and joint inversion problems.

## 5. REFERENCES

- [1] Adagunodo, T. A., L. A. Sunmonu, and A. A. Adeniji, An overview of magnetic method in mineral exploration[J], Journal of Global Ecology and Environment, 2015, 3(1):13-28.
- [2] XUE Ruijie, XIONG Jie, ZHANG Yue, WANG Rong, Magnetic Anomaly Inversion Based on Convolutional Neural Network[J], Geoscience, 2023, 37(1):173-183.
- [3] WEI C, LI X F, ZHEN X D. The group search based parallel algorithm for the serial Monte Carlo inversion method[J]. Applied Geophysics, 2010, 7(2), 127–134.
- [4] H Luo, Y Li, H Li, X Cui, Z Chen, Simulated annealing algorithm-based inversion model to interpret flow rate profiles and fracture parameters for horizontal wells in unconventional gas reservoirs[J], SPE Journal, 2021, 26(4):1679-1699.
- [5] da Conceição Batista, J., & Sampaio, E. E. S., Magnetotelluric inversion of one-and two-dimensional synthetic data based on hybrid genetic algorithms[J], Acta Geophysica, 2019, 67, 1365-1377.
- [6] Yadav, Apurwa, Kriti Yadav, and Anirbid Sircar, Feedforward neural network for joint inversion of geophysical data to identify geothermal sweet spots in Gandhar, Gujarat, India[J], Energy Geoscience, 2021, 2(3): 189-200.
- [7] XIONG Jie, LIU Caiyun, ZOU Changchun, The induction logging inversion based on particle swarm optimization[J], Geophysical and Geochemical Exploration, 2013, 37(6):1141-1145.
- [8] XIONG Jie, MENG Xiaohong, LIU Caiyun, PENG Miao, The induction logging inversion based on particle swarm optimization[J], Geophysical and Geochemical Exploration, 2012, 36(3):448-451.
- [9] Bouchaoui, Lyes, et al., Vertical electrical sounding data inversion using continuous ant colony optimization algorithm: A case study from Hassi R'Mel, Algeria[J], Near Surface Geophysics, 2022, 20(42): 419-439.
- [10] Dong, Shi, Ping Wang, and Khushnood Abbas, A survey on deep learning and its applications[J], Computer Science Review, 2021, 40: 100379.
- [11] ZHANG L Z, ZHANG G B, LIU Y, et al. Deep Learning for 3-D Inversion of Gravity Data[J]. IEEE Transactions on Geoscience and Remote Sensing, 2022, 60, 5905919.
- [12] Wang R, Xiong J, Liu Q, et al. Inversion of gravity anomalies based on a deep neural network[J], Geophysical and Geochemical Exploration, 2022, 46(2) :451–458.
- [13] Zhang ZH, LiaoXL, Cao YY, et al. Joint gravity and gravity gradient inversion based on deep learning[J], Chinese J. Geophys. (in Chinese), 2021, 64(4):1435-1452.